Electronic Supplementary Material

Phthalimide-based Unfused-Ring Non-fullerene Acceptors for Constructing Efficient Organic Solar Cells with High Open-Circuit Voltage

Baitian He,*[a] Luting Tang,[b] Xiuhua Huang,[a] Jinming Zhang,[a] Manjun Xiao,*[b] Guiting Chen,*[a] Chuanbo Dai[a]

[a] School of Chemistry and Environment, Guangdong Rare Earth Photofunctional Materials Engineering Technology Research Center, Jiaying University, Meizhou 514015, P. R. China

[b] College of Chemistry, Key Lab of Environment-Friendly Chemistry and Application (Ministry of Education), Xiangtan University, Xiangtan 411105, P. R. China

E-mail: baitian-he@foxmail.com

E-mail: xmj0704@xtu.edu.com

E-mail: cgt_jy@126.com

Experimental Section

***Materials*:** All solvents and reagents were purchased from commercial sources and used without further purification unless stated otherwise. The materials of PM6, 2-(3-oxo-2,3-dihydro-1H-inden-1-ylidene)malononitrile (IC), 2-(5,6-difluoro-3-oxo-2,3-dihydro-1H-inden-1-ylidene)malononitrile (IC-2F), 2-(5,6-dichloro-3-oxo-2,3-dihydro-1H-inden-1-ylidene)malononitrile (IC-2Cl) and compound M2 were purchased from Derthon OPV Co Ltd. Compound M1 was prepared according to the previously reported literature.[1]

Measurements: ^{1}H NMR and ^{13}C NMR spectra were recorded on a Bruker AV-400 MHz NMR spectrometer. Chemical shifts are reported in parts per million (ppm, δ). ^{1}H NMR and ^{13}C NMR spectra were referenced to tetramethylsilane (0 ppm) for $CDCl_3$. The molecular mass was confirmed using an Autoflex III matrix-assisted laser desorption ionization mass spectrometer (MALDI-TOF-MS). Elemental analysis were performed on a Elementar Vario EL cube. Thermogravimetric (TGA) measurements were carried out with a NETZSCH (TG209F3) apparatus at a heating rate of 20 °C min^{-1} under a nitrogen atmosphere. UV-vis absorption spectra were recorded on a SHIMADZU UV-3600 spectrophotometer. Cyclic voltammetry (CV) was carried out on a CHI660A electrochemical workstation with platinum electrodes at a scan rate of 50 mV s^{-1} against a platinum wire and saturated calomel electrodes (SCE) as reference electrode with nitrogen-saturated solution of 0.1 M tetrabutylammonium hexafluorophosphate in acetonitrile. The ferrocene/ferrocene (Fc/Fc^{+}) pair was used as an internal reference and the potential was calculated to be 0.39 V. The deposition of a copolymer on the electrode was done by the evaporation of a chloroform solution. Tapping-mode atomic force microscopy (AFM) images were obtained using a NanoScope NS3A system (Digital Instrument). Transmission electron microscopy (TEM) images were obtained using a JEM-2100F instrument.

DFT Calculations. The geometry was optimized with Density Functional Theory (DFT) using B3LYP hybrid functional with basis set 6-31g*.[2] Quantum-chemical

calculation was performed with the Spartan 10 software. All of the alkyl side chains were replaced with methyl groups to simplify the calculation.

Charge Carrier Mobility Measurements. The hole-only and electron-only devices were measured with device structures of ITO/PEDOT:PSS/PM6:Acceptor/MoO_3/Al and ITO/ZnO/ PM6:Acceptor /PFN-Br/Al, respectively. The mobility was determined by fitting the dark current to the model of a single-carrier SCLC, which is described by the following equation:

$$J = \frac{9}{8}\varepsilon_0 \varepsilon r \mu_0 \frac{V^2}{d^3}$$

where J is the current, μ_0 is the carrier mobility, ε_0 is the permittivity of free space, ε_r is the relative permittivity of the material, d is the thickness of the active layer, and V is the effective voltage.[3] The effective voltage can be obtained by subtracting the built-in voltage (V_{bi}) and the voltage drop (V_s) from the substrate's series resistance from the applied voltage (V_{appl}), i.e., $V = V_{appl} - V_{bi} - V_s$. The carrier mobility can be calculated from the slope of the $J^{1/2}$–V curves.

***Fabrication of Polymer Solar Cells and Characterization*:** The indium tin oxide (ITO) glass substrates were cleaned sequentially under sonication for 30 min with acetone, detergent, deionized water and isopropyl alcohol and then dried at 80 °C in baking oven overnight, followed by a plasma treatment for 4 min. The pre-cleaned ITO substrate were coated with PEDOT:PSS (filtered through a 0.45 μm PES filter) by spin-coating (3000 rpm. for 30 s, thickness of ~40 nm) and then baked at 150 °C for 15 min in air. Then, the substrates were transferred into a nitrogen (N_2) protected glovebox. The device configuration was ITO/PEDOT:PSS/PM6:Acceptor/PFN-Br/Al, and the active layers were spin coated from CF+0.5% CN solution containing PM6:Acceptor (weight ratio 1:1.2) to obtain thicknesses of ~100 nm. Thermal annealing of the blend films was carried out by placing them onto a hot plate in a nitrogen atmosphere. A 5 nm PFN-Br layer was then spin-coated from methanol solution onto the active layer. The thin films were transferred into a vacuum evaporator connected to the glove box, and Al (90 nm)

was deposited sequentially through a shadow mask under 10^{-7} Pa, with an active area of the cells of 0.04 cm^2.

The current–voltage (*J–V*) curves were measured on a computer-controlled Keithley 2400 sourcemeter under 1 sun, AM 1.5 G spectra from a class solar simulator (Taiwan, Enlitech), and the light intensity was 100 mW cm^{-2} as calibrated by a China General Certification Center certified reference monocrystal silicon cell (Enlitech). Before the *J–V* test, a physical mask of an aperture with a precise area of 0.04 cm^2 was used to define the device area. The EQE data were recorded with a QE-R3011 test system from Enli technology company (Taiwan).

Synthesis of the monomers

4,7-bis(4,4-bis(2-ethylhexyl)-4H-cyclopenta[2,1-b:3,4-b']dithiophen-2-yl)-2-(2-ethylhexyl)isoindoline-1,3-dione (M3)

A mixture of compound M1 (1.25 g, 3.00 mmol), M2 (3.90 g, 6.90 mmol), and $Pd(PPh_3)_4$ (138.67 mg, 0.12 mmol) in dry DMF (50 mL) was stirred at 120 °C under argon for 12 h. After cooling to room temperature, the mixture was poured into a solution of KF and extracted with DCM (50 mL × 3). The combined organic layer was dried over anhydrous Na_2SO_4, filtered, and evaporated to dryness. The residue was purified via column chromatography on silica gel (petroleum ether/DCM, 3:1) to afford a dark red oil (2.58 g, 2.43 mmol, 81%). ^{1}HNMR (400 MHz, $CDCl_3$): δ 7.86 (d, *J* = 1.1 Hz, 2H), 7.48-7.40 (m, 2H), 7.27-7.21 (m, 2H), 7.09 (s, 2H), 3.47 (d, *J* = 7.2 Hz, 2H), 2.01 – 1.82 (m, 8H), 1.86 (s, 1H), 1.34 – 1.23 (m, 8H), 0.99 – 0.86 (m, 36H), 0.74 – 0.60 (m, 30H).; ^{13}C NMR (101 MHz, $CDCl_3$): δ 165.21, 161.32, 157.41, 145.47, 143.64, 140.51, 138.75, 135.62, 131.75, 130.12, 127.32, 125.49, 54.65, 43.43, 43.55, 41.87, 38.12, 35.23, 34.22, 34.09, 30.43, 28.37, 28.52, 28.41, 27.36, 23.76, 23.01, 22.75, 14.05, 10.63, 10.59, 10.43.

6,6'-(6,7-difluoro-2,3-bis(3-(octyloxy)phenyl)quinoxaline-5,8-diyl)bis(4-(2-ethylhexyl)-4-(octan-3-yl)-4H-cyclopenta[2,1-b:3,4-b']dithiophene-2-

carbaldehyde) (M4)

Under nitrogen atmosphere, compound M3 (2.12 g, 2.00 mmol) was dissolved in anhydrous DMF (40 mL), Afterwards, the phosphorus oxychloride (1 mL) was dropwise added at 0°C, and the mixture was stirred at the room temperature for 30 min. Then, the mixture was heated to 80°C and stirred overnight. After cooling to room temperature, the mixture was poured into water to quench the reaction and extracted with extracted with DCM (50 mL × 3). The combined organic layer was dried over $MgSO_4$, filtered, and evaporated to dryness. The residue was purified via column chromatography on silica gel (petroleum ether/DCM, 1:1) to afford a organic oil (1.69 g, 1.52 mmol, 76%). ^{1}HNMR (400 MHz, $CDCl_3$): δ 9.87 (s, 2H), 7.88 (d, *J* = 1.1 Hz, 2H), 7.83 (s, 2H), 7.61 (s, 2H), 3.61 (d, *J* = 7.2 Hz, 2H), 2.03 – 1.84 (m, 8H), 1.84 (s, 1H), 1.36 – 1.25 (m, 8H), 1.00 – 0.87 (m, 36H), 0.75 – 0.61 (m, 30H).; ^{13}C NMR (101 MHz, $CDCl_3$): δ 182.58, 167.22, 162.05, 158.37, 147.30, 143.90, 141.30, 138.25, 135.02, 132.25, 130.62, 127.82, 125.79, 54.45, 43.21, 43.11, 42.11, 38.24, 35.29, 34.29, 34.16, 30.55, 28.58, 28.54, 28.45, 27.37, 23.90, 23.01, 22.75, 14.05, 10.63, 10.59, 10.43.

BPD-H

Compound M4 (167.51 mg, 0.15 mmol) and IC (87 mg, 0.45 mmol) were dissolved in the mixture of chloroform (30 mL) and anhydrous pyridine (0.2 mL) in a degassed two-neck round-bottom flask. The reaction was carried out at 60 °C for 24 hours. After removal of solvent under vacuum, the residue was purified via column chromatography on silica gel (petroleum ether/DCM, 1:1) to obtain a brown black solid (176.29 mg, 80% yield). ^{1}HNMR (400 MHz, $CDCl_3$): δ 8.95 (s, 2H), 8.69 (d, *J* = 7.2 Hz, 2H), 8.03 – 7.90 (m, 4H), 7.88 (s, 2H), 7.79 – 7.67 (m, 6H), 3.63 (d, *J* = 7.2 Hz, 2H), 2.15 – 1.95 (m, 8H), 1.85 (s, 1H), 1.43 – 1.23 (m, 8H), 0.95 (m, 38H), 0.70 (m, 28H). ^{13}C NMR (101 MHz, $CDCl_3$) δ 188.76, 187.37, 167.16, 165.03, 161.05, 159.78, 156.76, 144.28, 139.99, 139.41, 138.80, 138.26, 137.89, 137.01, 136.94, 135.08, 134.87, 134.20, 132.24, 128.19, 126.37, 125.19, 123.57, 120.90, 114.98, 68.19, 54.49, 43.19, 35.48, 35.41, 34.18, 34.07, 28.57, 28.44, 27.36, 22.79, 14.14, 10.71, 10.50. MS (MALDI-

TOF): calcd. for $C_{112}H_{124}F_2N_6O_4S_4$ (M^+): 1469.09, Found: 1468.3246. Anal. Calcd for $C_{92}H_{101}N_5O_4S_4$ (%): C, 75.22; H, 6.93; N, 4.77; O, 4.36; S, 8.73. Found: C, 75.25; H, 6.95; N, 4.46; O, 4.97; S, 8.43.

BPD-F

Compound M4 (167.51 mg, 0.15 mmol) and IC-2F (103.6 mg, 0.45 mmol) were dissolved in the mixture of chloroform (30 mL) and anhydrous pyridine (0.2 mL) in a degassed two-neck round-bottom flask. The reaction was carried out at 60 °C for 24 hours. After removal of solvent under vacuum, the residue was purified via column chromatography on silica gel (petroleum ether/DCM, 1:1) to obtain a brown black solid (175.68 mg, 76% yield). ^{1}H NMR (400 MHz, $CDCl_3$) δ 8.93 (s, 2H), 8.54 (dd, *J* = 10.0, 6.5 Hz, 2H), 8.01 – 7.92 (m, 2H), 7.89 (s, 2H), 7.69 (dd, *J* = 13.3, 5.8 Hz, 4H), 3.63 (d, *J* = 7.1 Hz, 2H), 2.12 – 1.96 (m, 8H), 1.85 (s, 1H), 1.41 – 1.26 (m, 8H), 1.09 – 0.89 (m, 36H), 0.70 (m, 30H). ^{13}C NMR (101 MHz, $CDCl_3$) δ 186.09, 166.99, 165.36, 165.30, 159.98, 158.49, 157.93, 155.70, 155.56, 153.15, 152.95, 144.91, 139.30, 138.79, 138.44, 136.55, 135.10, 134.51, 132.28, 128.35, 126.43, 126.31, 126.22, 119.93, 115.02, 114.80, 114.58, 114.54, 112.58, 112.39, 100.00, 68.54, 54.42, 43.39, 43.18, 35.51, 35.44, 34.21, 34.07, 30.56, 29.74, 28.56, 28.43, 27.35, 23.02, 22.78, 14.07, 10.65, 10.49. MS (MALDI-TOF): calcd. for $C_{112}H_{120}F_6N_6O_4S_4$ (M^+): 1541.05, Found: 1540.3085. Anal. Calcd for $C_{92}H_{97}F_4N_5O_4S_4$ (%): C, 71.71; H, 6.34; N, 4.54; O, 4.15; S, 8.32. Found: C, 71.67; H, 6.30; N, 4.14; O, 4.96; S, 8.12.

BPD-Cl

Compound M4 (167.51 mg, 0.15 mmol) and IC-2Cl (118.4 mg, 0.45 mmol) were dissolved in the mixture of chloroform (30 mL) and anhydrous pyridine (0.2 mL) in a degassed two-neck round-bottom flask. The reaction was carried out at 60 °C for 24 hours. After removal of solvent under vacuum, the residue was purified via column chromatography on silica gel (petroleum ether/DCM, 1:1) to obtain a black solid (173.54 mg, 72% yield). ^{1}H NMR (400 MHz, $CDCl_3$). δ 8.95 (s, 2H), 8.77 (s, 2H), 7.99 – 7.94 (m, 4H), 7.89 (s, 2H), 7.72 (s, 2H), 3.63 (d, J = 7.1 Hz, 2H), 2.06 – 2.00 (m, 8H),

1.85 (s, 1H), 1.39 – 1.25 (m, 8H), 1.02 – 0.88 (m, 36H), 0.76-0.63 (m, 30H).^{13}C NMR (101 MHz, $CDCl_3$) δ 186.17, 166.99, 165.59, 165.53, 160.12, 158.32, 145.44, 139.63, 139.36, 139.15, 138.79, 138.68, 136.05, 135.13, 132.22, 128.33, 126.88, 126.34, 125.01, 119.91, 114.64, 68.56, 54.45, 43.39, 43.20, 35.52, 35.45, 34.21, 34.06, 28.56, 28.43, 27.34, 23.92, 23.00, 22.79, 22.63, 14.07, 10.64, 10.49. MS (MALDI-TOF): calcd. for $C_{112}H_{120}Cl_4F_2N_6O_4S_4$ (M^+): 1606.86, Found: 1606.1898. Anal. Calcd for $C_{92}H_{97}C_{l4}N_5O_4S_4$ (%): C, 68.77; H, 6.08; N, 4.36; O, 3.98; S, 7.98. Found: C, 68.59; H, 6.01; N, 4.01; O, 4.52; S, 7.67.

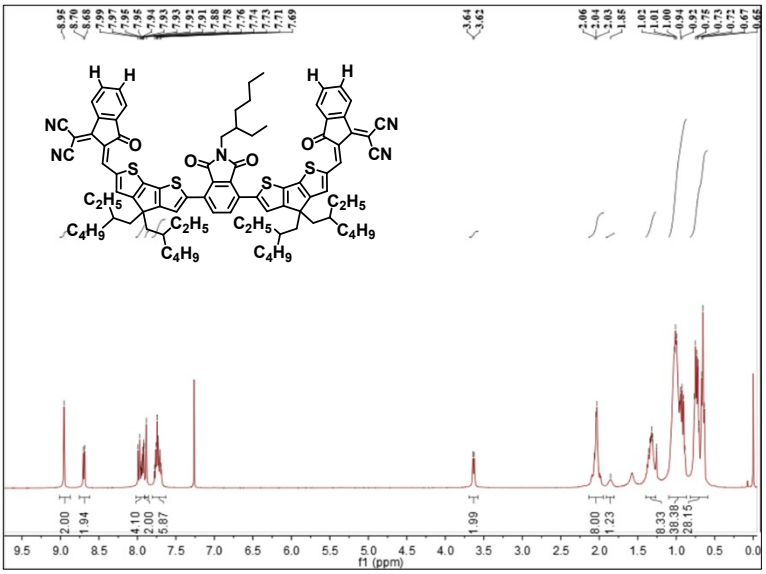

Fig. S1 ^{1}H NMR spectrum of BPD-H.

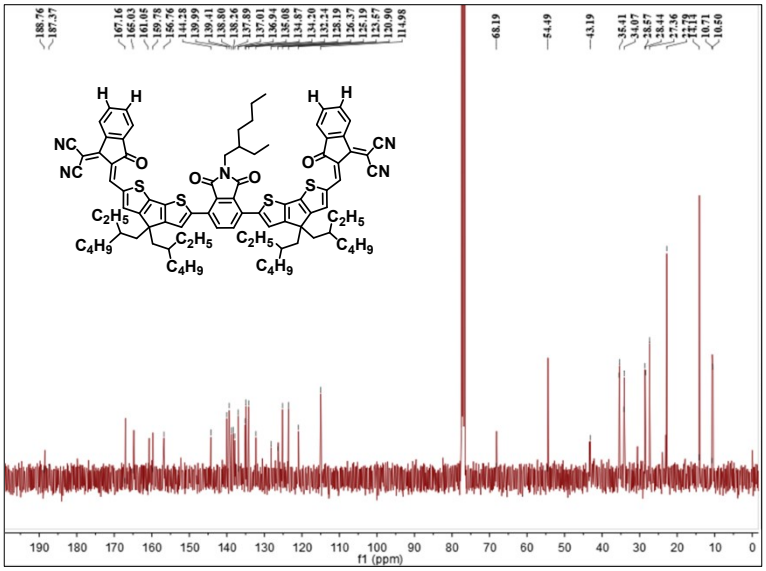

Fig. S2 ^{13}C NMR spectrum of BPD-H.

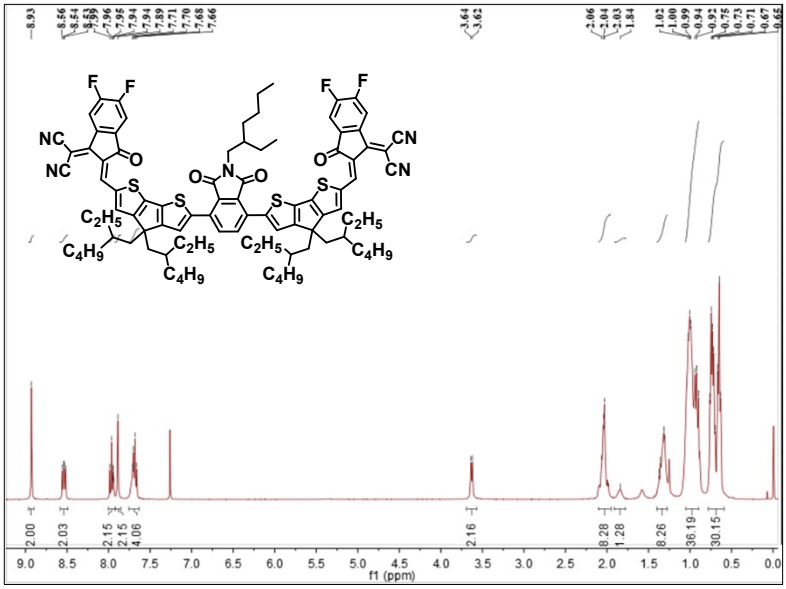

Fig. S3 ^{1}H NMR spectrum of BPD-F.

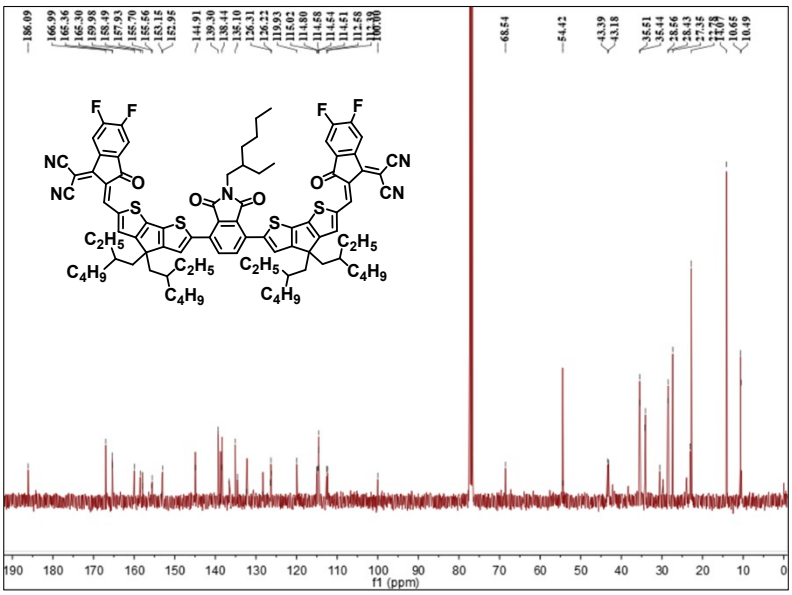

Fig. S4 ^{13}C NMR spectrum of BPD-F.

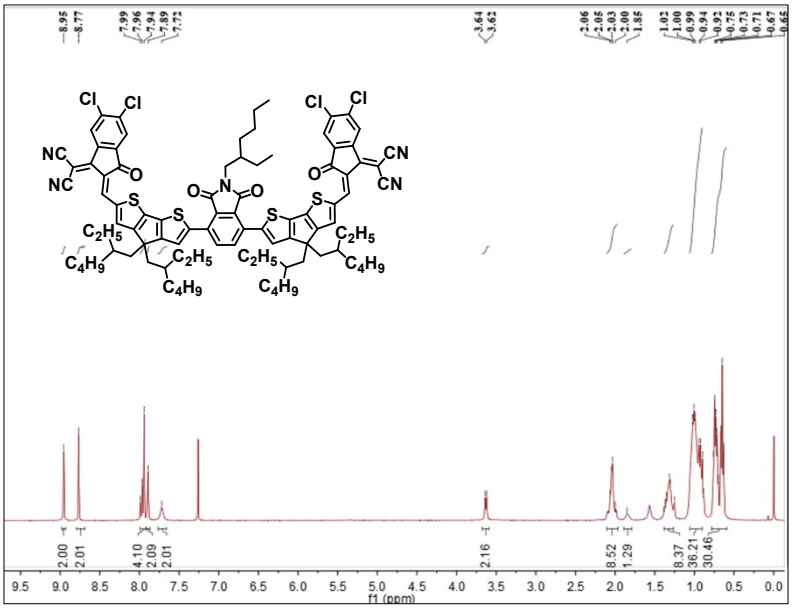

Fig. S5 ^{1}H NMR spectrum of BPD-Cl.

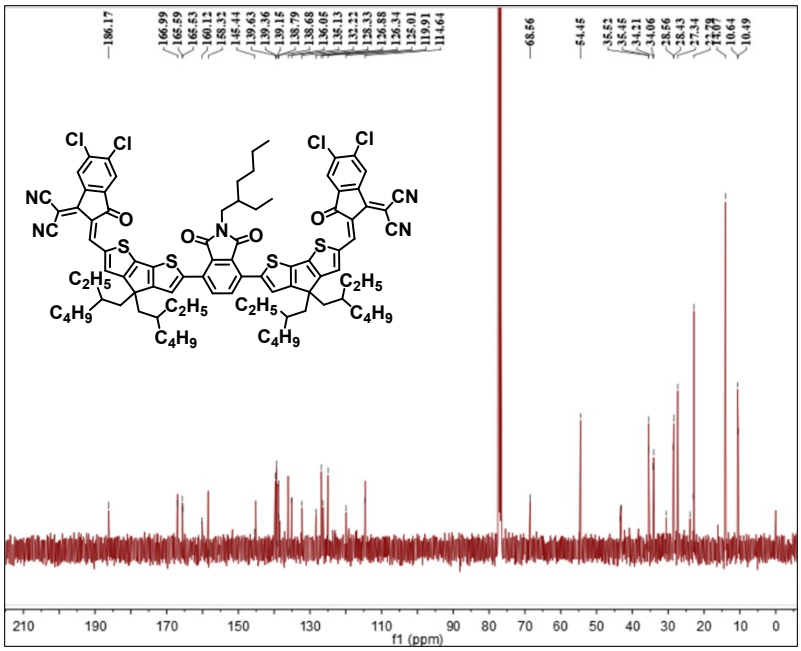

Fig. S6 ^{13}C NMR spectrum of BPD-Cl.

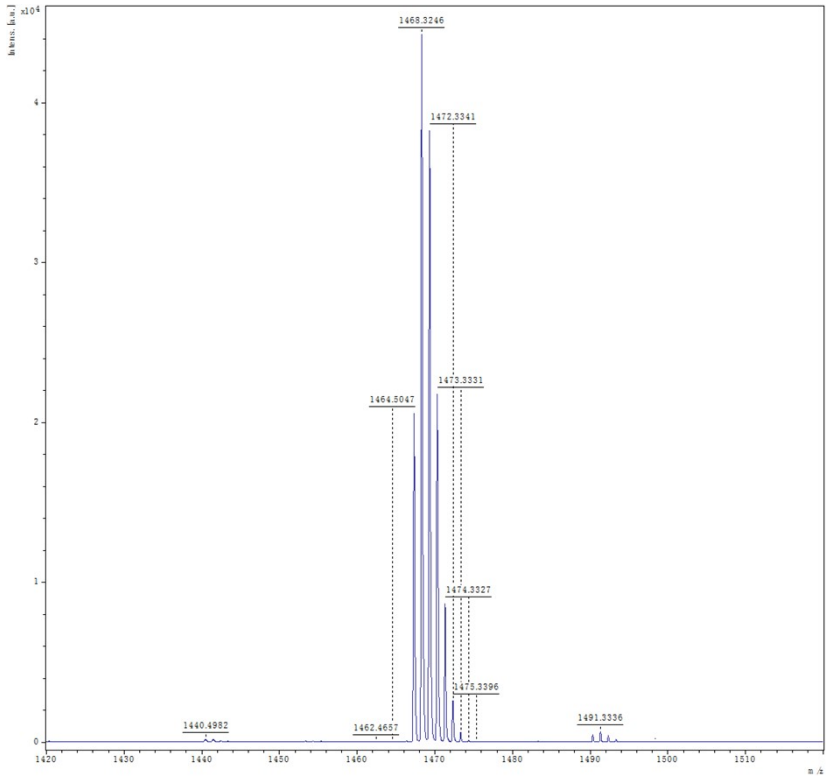

Fig. S7 MS spectrum (MALDI-TOF) of compound BPD-H.

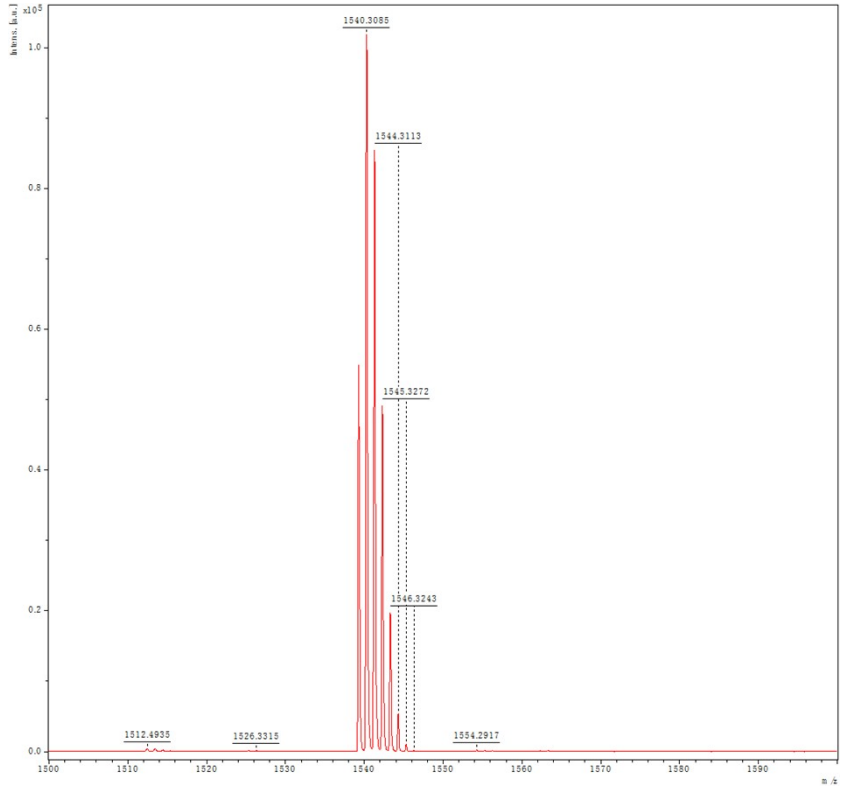

Fig. S8 MS spectrum (MALDI-TOF) of compound BPD-F.

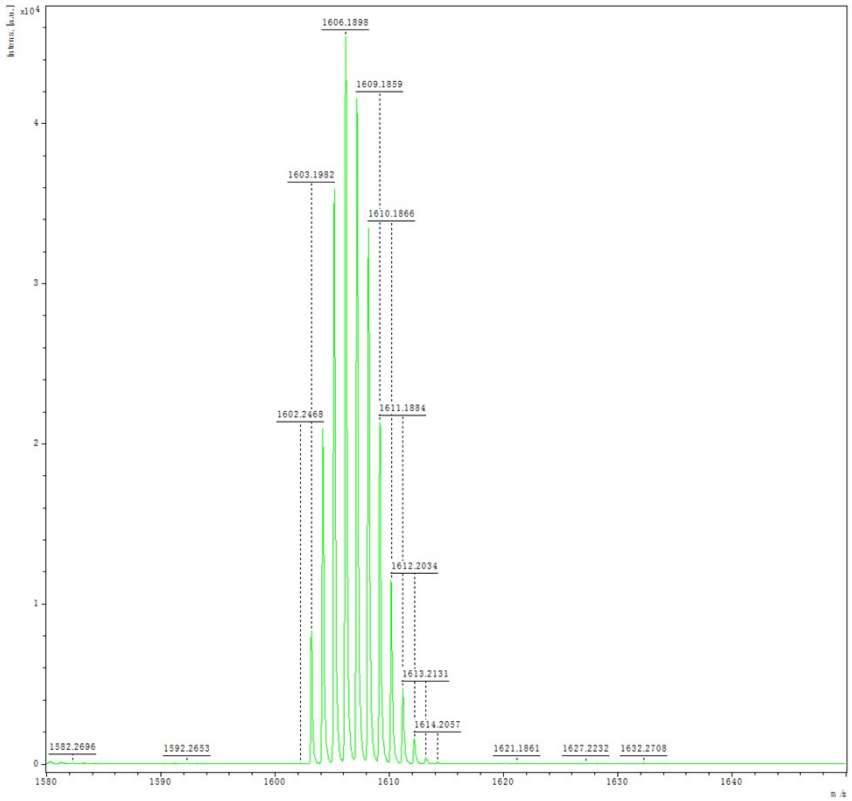

Fig. S9 MS spectrum (MALDI-TOF) of compound BPD-Cl.

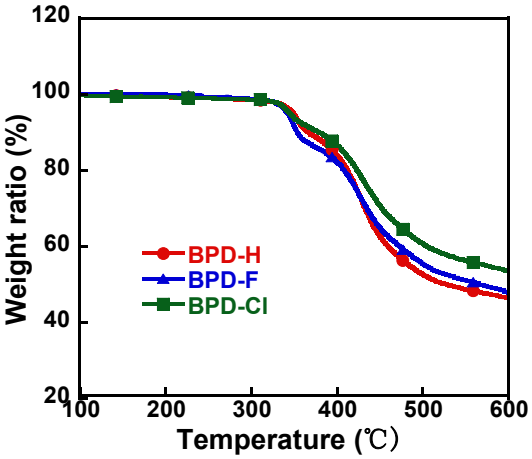

Fig. S10 TGA plot of UF-NFAs at a heating rate of 20 °C/min under a nitrogen atmosphere.

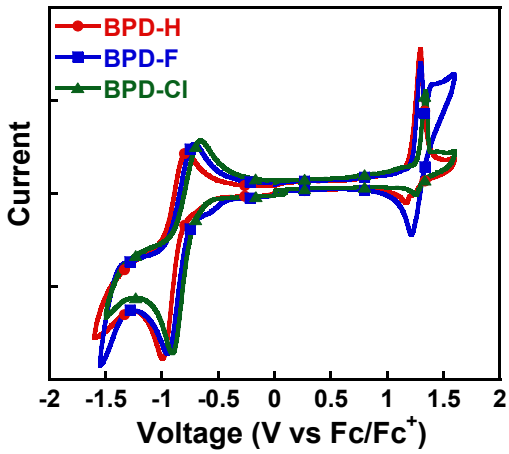

Fig. S11 CV curves of UF-NFAs with Fc/Fc^+ as the reference, using platinum electrodes as the working electrode, platinum wire as the counter electrode and SCE as the reference electrode, scan one cycle at the potential scanning rate of 50 $mV \cdot s^{-1}$ in 0.1 M tetrabutylammonium hexafluorophosphate (Bu_4NPF_6) acetonitrile solution.

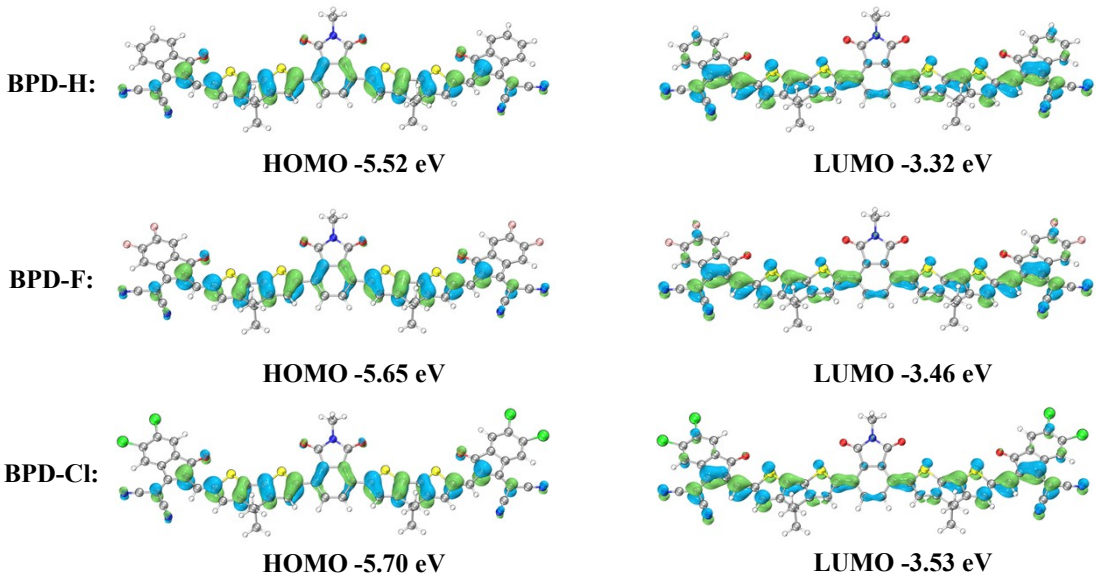

Fig. S12 The HOMO and LUMO energy levels of optimized geometries of BPD-X (X= H, F, Cl).

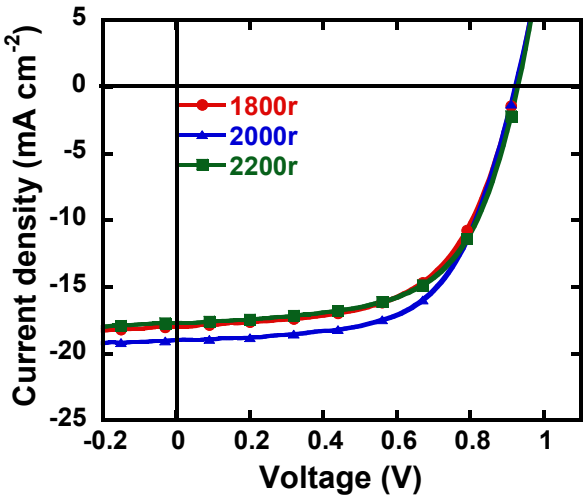

Fig. S13 *J–V* curves of OSCs under AM1.5 Illumination at 100 mW cm^{-2} with different speeding-coating rate of PM6:BPD-Cl.

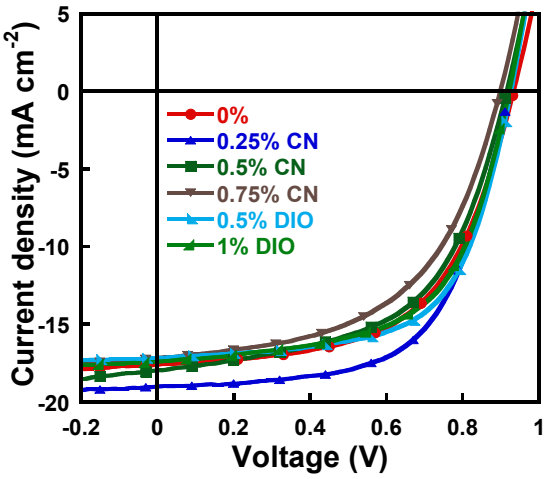

Fig. S14 *J–V* curves of OSCs under AM1.5 Illumination at 100 mW cm^{-2} with the PM6:BPD-Cl processed with various solvent additive.

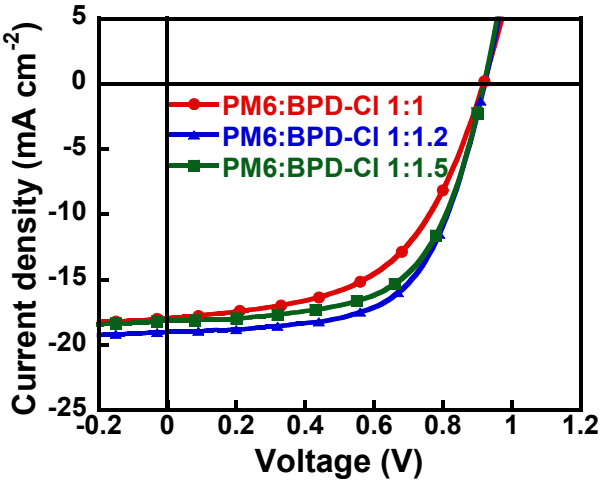

Fig. S15 *J–V* curves of OSCs under AM1.5 Illumination at 100 mW cm^{-2} with the PM6:BPD-Cl processed with different weight ratios.

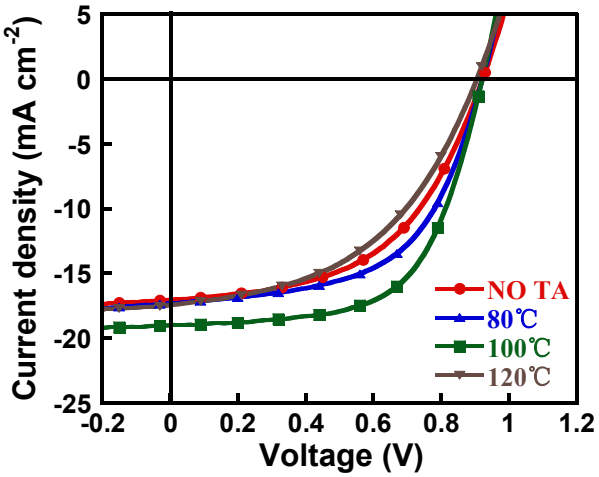

Fig. S16 *J–V* curves of OSCs under AM1.5 Illumination at 100 mW cm^{-2} with the

PM6:BPD-Cl processed with different thermal annealing temperature.

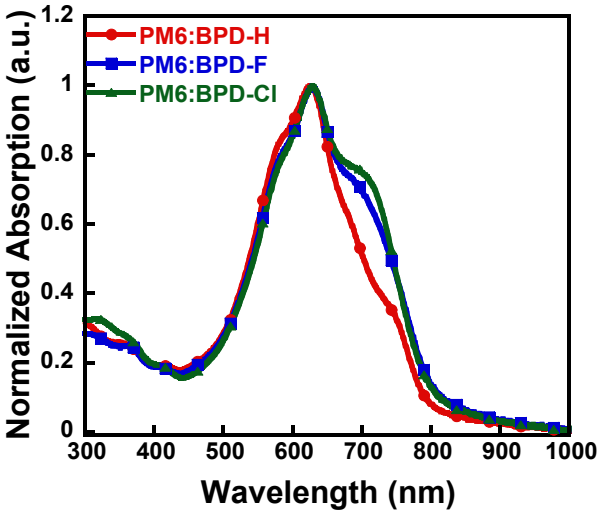

Fig. S17 Absorption spectra of PM6:BPD-X blended films.

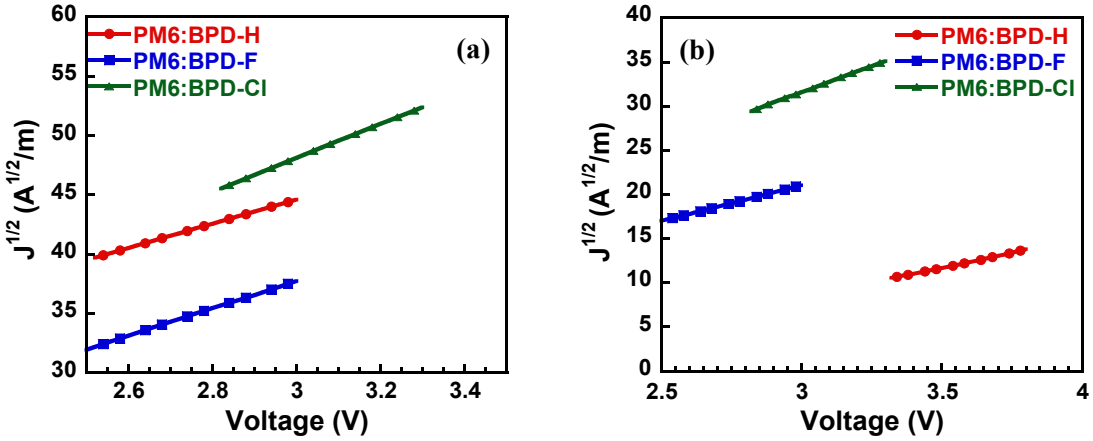

Fig. S18 $J^{1/2}$~(V_{appl}-V_{bi}-V_s) characteristics of hole-only (a) and electron-only (b) devices.

Table S1 Device performance of the OSCs based on PM6: BPD-Cl with different spin coating speed under AM1.5 Illumination at 100 mW cm^{-2}.

Blend film [a]	Speed (rpm)	V_{OC} (V)	J_{SC} (mA cm^{-2})	FF (%)	PCE (%)
PM6: BPD-Cl	1800	0.923	17.99	59.31	9.85
	2000	0.922	18.99	61.28	10.72
	2200	0.920	17.48	58.66	9.44

Table S2 Device performance of the OSCs based on PM6: BPD-Cl with different D/A ratios under AM1.5 Illumination at 100 mW cm^{-2}.

Blend film [a]	D/A (wt/wt)	V_{OC} (V)	J_{SC} (mA cm^{-2})	FF (%)	PCE (%)
PM6: BPD-Cl	1:1.1	0.917	17. 92	53.74	8.84
	1:1.2	0.922	18.99	61.28	10.72
	1:1.5	0.919	18.13	60.88	10.15

[a] All of the blend films are processed by CF.

Table S3 Device performance of the OSCs based on PM6: BPD-Cl with different thermal annealing under AM1.5 Illumination at 100 mW cm^{-2}.

Blend film [a]	thermal annealing	V_{OC} (V)	J_{SC} (mA cm^{-2})	FF (%)	PCE (%)
PM6: BPD-Cl	NO	0.923	17.04	51.65	8.12
	80℃	0.922	17. 30	56.51	9.02
	100℃	0.922	18.99	61.28	10.72
	120℃	0.906	17.45	47.40	7.49

[a] All of the blend films are processed by CF with Donor : Acceptor =1:1.2

Table S4 Device performance of the OSCs based on PM6: BPD-Cl processed with different additive under AM1.5 Illumination at 100 mW cm^{-2}.

Blend film [a]	Additive	V_{OC} (V)	J_{SC} (mA cm^{-2})	FF (%)	PCE (%)
PM6: BPD-Cl	NO	0.927	17.34	57.19	9.19
	0.25% CN	0.922	18.99	61.28	10.72
	0.5% CN	0.914	17.96	55.35	9.09
	0.75% CN	0.898	17.16	53.55	8.25

	0.5% DIO	0.926	17.14	62.70	9.96
	1.0% DIO	0.921	17.38	59.54	9.53

[a] Donor : Acceptor =1:1.2, All of the blend films are processed by CF with thermal annealing at 100 ℃.

Table S5 Relevant parameters obtained from J_{ph}–V_{eff} curves.

Blend films [a]	J_{ph} [b] (mA cm^{-2})	J_{sat} (mA cm^{-2})	P (E,T)[b]	L (nm)
PM6: BPD-H	14.71	16.74	88.0%	100
PM6: BPD-F	15.61	16.86	92.6%	100
PM6: BPD-Cl	18.73	19.54	96.0%	100

[a] Donor : Acceptor =1:1.2; all of the blend films are processed by CF with 0.25 vol% CN. [b] At the condition of $V_{eff} = V_0 - V_{appl}$ ($V_{appl} = 0$, under short-circuit condition).

Reference

[1] J. Yu, J. Yang, X. Zhou, S. Yu, Y. Tang, H. Wang, J. Chen, S. Zhang, X. Guo, *Macromolecules*, 2017, **50**, 8928–8937.

[2] S. Pang, X. Zhou, S. Zhang, H. Tang, S. Dhakal, X. Gu, C. Duan, F. Huang, Y. Cao, *ACS Appl. Mater. Interfaces*, 2020, **12**, 16531–16540.

[3] H. Yu, Z. Qi, X. Li, Z. Wang, W. Zhou, H. Ade, H. Yan, and K. Chen, *Sol. RRL*, 2020, **4**, 2000421.